PHYSICAL REVIEW A VOLUME 36, NUMBER 4 AUGUST 15, 1987

Angular correlation of two electrons on a sphere

P. C. Ojha and R. S. Berry
Department of Chemistry, University of Chicago, 5735 South Ellis Avenue, Chicago, Illinois 60637

(Received 4 March 1987)

As an approach to the electronic structure of the doubly excited and other highly correlated states of atoms, we consider the angular correlation of two electrons on a sphere of radius R. The Hamiltonian is scaled by a factor R^2 and the parameter R is reinterpreted as the strength of electronic repulsion. The scaled Hamiltonian H_S is the sum of an analytically solvable Hamiltonian H_0+V_M and a perturbation $\Delta H_1+\Delta H_2$ which becomes negligible as $R\to\infty$. The spectrum of H_0+V_M therefore approaches the spectrum of H_S in the asymptotic limit. The eigenfunctions of H_0+V_M show a transition from weak correlation at small R to strong correlation and "molecular" motion at large R.

I. INTRODUCTION

The independent-particle model has long been taken as the starting point for the description of the electronic states of atoms. It is particularly appropriate for Rydberg states where the motion of the Rydberg electron, by virtue of its distance from the ionic core, is not correlated with the motion of the core electrons. However, during the last few years, exceptions to this picture have emerged. Kellman and Herrick[1] discovered that the energy levels of the intrashell doubly excited states of helium (He**) fall into patterns strikingly reminiscent of the rovibrational spectrum of a linear triatomic molecule $Y—X—Y$. The implication is that the Coulomb repulsion of the electrons tends to keep them away from each other and on opposite sides of the nucleus. The resulting motion is therefore highly correlated. This picture has been supported[2] by examination of conditional probability distributions based on well-converged wave functions for various states of He** and its isoelectronic ions, for the alkaline-earth-metal atoms, and for the bound states of alkali-metal negative ions where the dynamics are essentially those of two electrons with comparable degrees of radial excitation moving in the field of an ionic core of low net charge.

Such strongly correlated motion depends sensitively on two factors. The first is the relative degree of radial excitation of the electrons. The motion evolves from being correlated to being uncorrelated as the disparity between the radial excitation of the electrons (the mismatch between their principal quantum numbers) increases. The second is the competition between core attraction and electronic repulsion. If the core charge is low, electronic repulsion dominates and the motion is correlated. In contrast, if the core charge is high, core attraction dominates and the motion is uncorrelated.

A proper *ex ante* delineation of when to expect collective or independent-particle-like character of the electronic motion is still an unsolved problem. A simplified model which should retain the relevant essential features of atoms constrains the electrons to lie on the surfaces of two concentric spheres of radii R_1 and R_2, allowing rotations of the two electrons (in the independent-particle picture) or bending and rigid-body rotations (in the collective picture). This model thus eliminates radial motion and provides a point of stable equilibrium at $\theta=\pi$. (θ is the angle between the radius vectors.) It is argued that the ratio R_2/R_1 in the model corresponds to the relative degree of radial excitation of the electrons. Thus $R_2/R_1=1$ corresponds to the intrashell doubly excited states whereas $R_2/R_1 \gg 1$ corresponds to the Rydberg states. Fixing R_2/R_1 and increasing the radii in proportion corresponds to weakening the core attraction. The angular correlation in this model has been explored numerically for some selected values of the radii by Ezra and Berry.[3,4] More recently, Nikitin and Ostrovsky[5] have tried to obtain approximate formulas for the energy levels. A slight variant of this model has also emerged as one natural approximation in a sequence of successively more accurate descriptions of vibrational and rotational motion in triatomic molecules such as H_2O.[6]

In this paper we further analyze the simpler model system when the two radii are equal, $R_1=R_2=R$. The Hamiltonian is quite simple:

$$H(R)=\frac{l_1^2}{2R^2}+\frac{l_2^2}{2R^2}+\frac{1}{R\sqrt{2(1-\cos\theta)}}\ , \tag{1.1}$$

where the first two terms give the kinetic energy of the electrons on the sphere and the last term represents their Coulomb interaction. It is preferrable to scale it by the factor R^2 and work with the scaled Hamiltonian,

$$H_S(R)=\tfrac{1}{2}l_1^2+\tfrac{1}{2}l_2^2+\frac{R/\sqrt{2}}{\sqrt{(1-\cos\theta)}}\ . \tag{1.2}$$

The radius R is now reinterpreted as the strength of the electronic repulsion. It is obvious that for small R (≈ 0) the motion will be weakly correlated whereas for large R ($\gg 1$) it will be strongly correlated. This transition in the nature of angular correlation as the parameter R is increased from zero is elucidated in the rest of this paper.

The problem is best regarded in the Euler angle coordinates[7,8] which are summarized in Appendix A. A quantum number K which gives the projection of the total angular momentum on an internal axis (parallel to the difference of the unit vectors $\hat{\mathbf{r}}_1-\hat{\mathbf{r}}_2$), and a symmetry label ($\pm$) related to the parity and exchange symmetry of the wave function, are introduced.

The heart of the matter is addressed in Sec. II. There we show that the Hamiltonian (1.2) may be broken into an analytically solvable Hamiltonian H_0+V_M and a perturbation $\Delta H_1+\Delta H_2$. The eigenfunctions of H_0+V_M are separable in the interelectronic angle θ and the Euler angles (α,β,γ). Consequently, they are characterized by the bending-vibrational quantum number v, the projection of the angular momentum K, and the symmetry label ($\pm$), besides the usual term symbol ${}^{2S+1}L^{\pi}$. The spectrum of H_0+V_M displays rovibrational progressions and "K doubling" for $K\geq 2$. (This symmetry is weakly broken when $K=1$.) The evolution from weak to strong correlation is also demonstrated and quantified.

The perturbation ΔH_1 mixes states with different v but preserves the quantum number K whereas ΔH_2 mixes different K values also. However, we are able to show that asymptotically (as $R\to\infty$), the entire perturbation $\Delta H_1+\Delta H_2$ is negligible. Hence the spectrum of H_0+V_M approaches that of H_S in the asymptotic limit as $R\to\infty$. Numerical evidence is then presented that $R=16$ a.u. marks the onset of the strong correlation regime for the states considered in this paper. We conclude Sec. III with some remarks regarding the possibility of extending this work and eventually integrating it into a comprehensive view of electron correlation in the doubly excited states of atoms.

II. THE NATURE OF THE SCHRÖDINGER EQUATION AND ITS SOLUTION

We next rewrite the Hamiltonian (1.2) in the Euler angle coordinates:

$$H_S=H_0+V_C+\Delta H_2\ , \tag{2.1a}$$

$$\begin{aligned}H_0=&-(1-\xi^2)\frac{d^2}{d\xi^2}+2\xi\frac{d}{d\xi}+\frac{1}{4(1-\xi)}(\mathbf{L}^2-L_{y'}^2)\\&+\frac{1}{2(1+\xi)}L_{y'}^2+\frac{1}{16}\frac{(1+\xi)}{(1-\xi)}(L'^2_{+}+L'^2_{-})_{\text{diag}}\\&+\tfrac{1}{8}(L^2-L_{y'}^2)\ ,\end{aligned} \tag{2.1b}$$

$$V_C=\frac{R/\sqrt{2}}{(1-\xi)^{1/2}}\ , \tag{2.1c}$$

$$\Delta H_2=\frac{1}{16}\frac{(1+\xi)}{(1-\xi)}(L'^2_{+}+L'^2_{-})_{\text{off}}\ . \tag{2.1d}$$

The operators $L'_{\pm}=-L_{x'}\mp iL_{z'}$ are the raising and lowering operators for the angular momentum components $L_{y'}$. Recall that the eigenfunctions of H_S which have definite parity and exchange symmetry are of the form $\sum_{K=K_0}^{L}F_K^{\pm}(\xi)\,|\,LMK(\pm)\rangle$, where K is incremented by 2 in the sum. The following selection rule is evident:

$$\begin{aligned}&\langle LMK_2(\pm)\,|\,L'^2_{+}+L'^2_{-}\,|\,LMK_1(\pm)\rangle\\&\quad\neq 0\ \text{ if }\ |K_1-K_2|=2\ \text{ or }\ K_1=K_2=1\ ,\\&\quad=0\ \text{ otherwise }.\end{aligned}$$

The diagonal part (in the index K) of the matrix, indicated by the subscript "diag," is nonzero only if $K=1$ and this is included in the noninteracting Hamiltonian H_0 of (2.1b). The remaining off-diagonal part, indicated by the subscript "off," is displayed separately because we expect that the states having strongly correlated motion at large R, by virtue of the localization of their wave functions near $\xi=-1$, will be well characterized by the quantum number K. We will show later that this is indeed the case and the symmetry-breaking term ΔH_2 is small and may be treated as a perturbation.

Let us then disregard ΔH_2 for the moment and consider the eigenfunctions of the operator H_0+V_C. These are required to be regular at $\xi=\pm 1$ and this condition can be satisfied only at a discrete set of energies. The Hamiltonian is now separable in the coordinate ξ and the Euler angles (α,β,γ). Consequently, anticipating the quantum number[9] v which gives the number of nodes in ξ,

$$\Psi^{\pm}_{vLMK}(\xi)=\Phi^{\pm}_{vLMK}(\xi)\,|\,LMK(\pm)\rangle\ , \tag{2.2a}$$

where the function $\Phi^{\pm}_{vLMK}(\xi)$ satisfies the following differential equation:

$$\left[-(1-\xi^2)\frac{d^2}{d\xi^2}+2\xi\frac{d}{d\xi}+\frac{1}{4}\frac{[L(L+1)-K^2]}{(1-\xi)}+\frac{1}{2}\frac{K^2}{(1+\xi)}+\frac{1}{16}\frac{(1+\xi)}{(1-\xi)}G(K)+\tfrac{1}{8}[L(L+1)-K^2]+\frac{R/\sqrt{2}}{(1-\xi)^{1/2}}-E\right]\Phi^{\pm}_{vLMK}(\xi)=0\ . \tag{2.2b}$$

In this equation $G(K)$ is the diagonal matrix element of $(L'^2_{+}+L'^2_{-})$ and as discussed earlier

$$\begin{aligned}G(K)&=\pm L(L+1),\quad K=1\ (\pm)\\&=0\ \text{ otherwise }.\end{aligned} \tag{2.2c}$$

Notice that (2.2b) is a second-order differential equation of the form

$$\left[\frac{d^2}{d\xi^2}+p(\xi)\frac{d}{d\xi}+q(\xi)\right]f(\xi)=0\ , \tag{2.3}$$

where $p(\xi)$ has simple poles at $\xi=\pm 1$ and $q(\xi)$ has a double pole at $\xi=-1$ but a branch point singularity at

$\xi=1$ arising from the Coulomb interaction. The solutions therefore have an essential singularity at $\xi=1$ and cannot be obtained analytically.

One can get rid of the troublesome branch point by the simple strategem of redefining the independent variable $t=\sqrt{1-\xi}$. This gives an eigenvalue equation of form (2.3) where the only singularities of $p(t)$ and $q(t)$ are, respectively, simple and double poles at $t=0$, $\pm\sqrt{2}$. These are thus the regular singular points of the differential equation. Unfortunately, there is an additional regular singular point at $t=\infty$. Such equations with four regular singular points are named after Heun[10] who was the first person to study them nearly 100 years ago. The most convenient method for solving them is by expanding the solution in a complete set of Jacobi polynomials. Although the fact that the expansion coefficients satisfy a three-term recursion relation affords some theoretical insight into the nature of the solution, this method is essentially numerical and unsuitable for our purpose.

The preceding remarks do imply that there exists a solution $\phi_1(\xi)$ which may be expanded in a power series in $(1-\xi)^{1/2}$ near the point $\xi=1$:

$$\phi_1(\xi)=(1-\xi)^{s_1}\sum_{\nu} a_\nu(1-\xi)^{\nu/2} , \tag{2.4a}$$

where s_1 is a root of the second-order indicial equation. The difficulty is that one does not know the behavior of $\phi_1(\xi)$ near $\xi=-1$ and its connection with another solution $\phi_2(\xi)$ which possesses an expansion in powers of $(1+\xi)$ near $\xi=-1$:

$$\phi_2(\xi)=(1+\xi)^{s_2}\sum_{\nu} b_\nu(1+\xi)^{\nu} , \tag{2.4b}$$

where s_2 is a root of the indicial equation at $\xi=-1$. This inability to connect the simply-behaved solutions at the regular singular points $\xi=\pm 1$ makes it impossible to identify analytically the eigenvalues which are determined by the condition that $\phi_1(\xi)$ and $\phi_2(\xi)$ be identical.

We circumvent this difficulty by approximating the Coulomb potential by a model potential,

$$V_M(\xi)=\frac{\lambda_1}{1-\xi}+\lambda_2,\quad \lambda_1=R/2,\quad \lambda_2=R/4 . \tag{2.5}$$

The parameters λ_1 and λ_2 are determined by the pair of conditions

$$V_M(\xi=-1)=V_C(\xi=-1) , \tag{2.6a}$$

$$\left.\frac{dV_M}{d\xi}\right|_{\xi=-1}=\left.\frac{dV_C}{d\xi}\right|_{\xi=-1} . \tag{2.6b}$$

Thus, near $\xi=-1$, $V_M(\xi)$ differs from $V_C(\xi)$ only in second order. Correspondingly, in terms of the angle θ, $V_M(\theta)$ differs from $V_C(\theta)$ near $\theta=\pi$ in fourth order only, and like $V_C(\theta)$, $V_M(\theta)$ is at its minimum at this point. The illustration in Fig. 1 shows that the Coulomb interaction is approximated very closely by the model potential over the range $\pi/2\le\theta\le\pi$. The eigenstates of V_M localized in this region will therefore be good approximations to such states of the Coulomb interaction.

We therefore rewrite

$$H_S=H_0+V_M+\Delta H_1+\Delta H_2 , \tag{2.7a}$$

with

$$\Delta H_1=V_C-V_M , \tag{2.7b}$$

and seek eigenfunctions of the model Hamiltonian $H_M=H_0+V_M$. It will be shown later that like ΔH_2, ΔH_1 also constitutes a small perturbation to the states of interest.

A. The spectrum of H_0+V_M

The eigenfunctions of H_0+V_M are also of the form (2.2a) with the difference that $\Phi^{\pm}_{\nu LMK}(\xi)$ must satisfy the following differential equation:

$$\left[-(1-\xi^2)\frac{d^2}{d\xi^2}+2\xi\frac{d}{d\xi}+\frac{1}{4}\frac{[L(L+1)-K^2+2R]}{(1-\xi)}+\frac{1}{2}\frac{K^2}{(1+\xi)}+\frac{1}{16}\frac{(1+\xi)}{(1-\xi)}G(K)-\left[E_\nu-\frac{1}{8}[L(L+1)-K^2]-R/4\right]\right]\Phi^{\pm}_{\nu LMK}(\xi)=0 . \tag{2.8}$$

This equation has three regular singular points at $\xi=\pm 1,\infty$ and its solution is therefore given by the Gauss hypergeometric function.[11] At selected energies it reduces to a Jacobi polynomial which is regular at $\xi=\pm 1$.

We define the parameter

$$\alpha=[\tfrac{1}{2}L(L+1)-\tfrac{1}{2}K^2+R]^{1/2},\quad K\neq 1;\pm \tag{2.9a}$$

$$=[(\tfrac{1}{2}\pm\tfrac{1}{4})L(L+1)-\tfrac{1}{2}K^2+R]^{1/2},\quad K=1;\pm \tag{2.9b}$$

in terms of which the energy levels are given by the following simple formula:

$$E_\nu=[\nu+\tfrac{1}{2}(\alpha+K)][\nu+\tfrac{1}{2}(\alpha+K)+1]+\tfrac{1}{4}\alpha^2\quad\text{when } K\neq 1;\pm \tag{2.10a}$$

$$=[\nu+\tfrac{1}{2}(\alpha+K)][\nu+\tfrac{1}{2}(\alpha+K)+1]+\tfrac{1}{4}\alpha^2\mp\tfrac{1}{8}L(L+1)\quad\text{when } K=1;\pm . \tag{2.10b}$$

The corresponding normalized eigenfunctions are

$$\Phi^{\pm}_{\nu LMK}(\xi)=N^{\alpha,K}_{\nu}(1-\xi)^{\alpha/2}(1+\xi)^{K/2}P^{\alpha,K}_{\nu}(\xi) , \tag{2.11}$$

where $P_v^{\alpha,K}(\xi)$ is a Jacobi polynomial[12] and $N_v^{\alpha,K}$ is its normalization factor given in (2.8b). Note that if $K\neq 1$, the parameter α does not depend on the symmetry label $(\pm)$. The energy levels are therefore doubly degenerate (K doubling) when $K\geq 2$. When $K=1$, this degeneracy is weakly broken by the diagonal part of the operator $(L'^2_{+}+L'^2_{-})$ which is retained in the Hamiltonian H_0+V_M through (2.1a). There is an additional "accidental" degeneracy between the ${}^3P^o$ levels $[v,K=0,+]$ and ${}^1D^e$ and ${}^3D^o$ levels $[v-1,K=2,\pm]$ which arises from the numerical accident that the corresponding α parameters are identical. Permissible quantum numbers K, the symmetry labels $(\pm)$, and the corresponding values of α are listed for several terms ${}^{2S+1}L^{\pi}$ in Table I.

The rovibrational progressions identified in the numerical study of Ezra and Berry[3] are encapsulated in Eq. (2.10). A rotor series is characterized by fixed values of v and K. Displaying the L dependence of the energy levels doubly degenerate for $K>1$, we have

$$E=\tfrac{1}{4}L(L+1)+\tfrac{1}{2}(2v+K+1)[\tfrac{1}{2}L(L+1)-\tfrac{1}{2}K^2+R]^{1/2}+[v(v+1)+\tfrac{1}{2}(2v+1)K+\tfrac{1}{2}R],\quad \text{when } K\neq 1;\pm \tag{2.12a}$$

$$=\tfrac{1}{4}L(L+1)+\tfrac{1}{2}(2v+K+1)[(\tfrac{1}{2}\pm\tfrac{1}{4})L(L+1)-\tfrac{1}{2}K^2+R]^{1/2}+[v(v+1)+\tfrac{1}{2}(2v+1)K+\tfrac{1}{2}R]\quad \text{when } K=1;\pm\ . \tag{2.12b}$$

In either case the strong L dependence comes from the first term generating the rotor series. The weaker modulation from the second term becomes important only at large L.

A vibrational series is characterized by fixed values of L and K but a varying bending-vibrational quantum number v. The spacing between consecutive members of the series is

$$E_{v+1}-E_v=2(v+1)+K+[\tfrac{1}{2}L(L+1)-\tfrac{1}{2}K^2+R]^{1/2}\quad \text{when } K\neq 1;\pm \tag{2.13a}$$

$$=2(v+1)+K+[(\tfrac{1}{2}\pm\tfrac{1}{4})L(L+1)-\tfrac{1}{2}K^2+R]^{1/2}\quad \text{when } K=1;\pm\ . \tag{2.13b}$$

The v dependence reflects the anharmonic nature of the bending vibration which is important even for the low-lying levels. This suggests that the harmonic approximation may be inadequate in describing the bending vibration of the doubly excited states of atoms or even of non-rigid linear triatomic molecules such as CH_2.

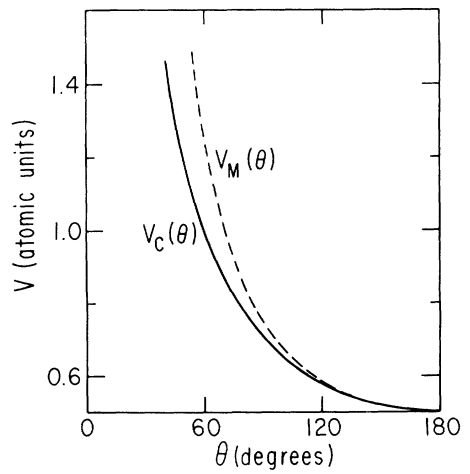

FIG. 1. A comparison of the Coulomb potential $V_C(\theta)=1/\sqrt{2(1-\cos\theta)}$ and the model potential $V_M(\theta)=1/2(1-\cos\theta)+\frac{1}{4}$. Note that the model potential closely approximates the Coulomb potential in the region $\pi/2\leq\theta\leq\pi$.

The localization of the wave function near $(\xi=-1)$ comes from the term $(1-\xi)^{\alpha/2}$ which is part of the weight function of the Jacobi polynomial. It is quantified most conveniently by the expectation value $\langle 1+\xi\rangle$ and the root-mean-square deviation $\langle\Delta(1+\xi)\rangle_{\text{rms}}=(\langle(1+\xi)^2\rangle-\langle 1+\xi\rangle^2)^{1/2}$. For all energy levels

$$\langle 1+\xi\rangle=\frac{1}{(2v+\alpha+1)}\left[\frac{2(v+K+1)(v+\alpha+K+1)}{(2v+\alpha+K+2)}+\frac{2v(v+\alpha)}{(2v+\alpha+K)}\right]. \tag{2.14a}$$

This reduces to a particularly simple form for the primary rotor series:

$$\langle 1+\xi\rangle=\frac{2}{(\alpha+2)}\quad \text{when } v=0,\ K=0\ . \tag{2.14b}$$

The exact general expression for the root-mean-square deviation of this expectation value is lengthy and not very illuminating. We quote the result for the primary rotor series

$$\langle\Delta(1+\xi)\rangle_{\text{rms}}=\frac{2}{(\alpha+2)}\left[\frac{\alpha+1}{\alpha+3}\right]^{1/2}\quad \text{when } v=0,\ K=0\ , \tag{2.15a}$$

and the (large-α) asymptotic form for the general case

$$\lim_{\alpha\to\infty}\langle\Delta(1+\xi)\rangle_{\text{rms}}=\frac{2}{\alpha}[3v^2+(3v+1)(K+1)]^{1/2}+O(1/\alpha^2)\ . \tag{2.15b}$$

The localization of the wave function near $\xi=-1$ with increasing R (recall that α goes to $\sqrt{R}$ as $R\to\infty$) is evident from Eqs. (2.14) and (2.15).

In concluding Sec. II A, note that the separation between any two levels characterized by the same quantum numbers L and K and the symmetry label $(\pm)$,

$$E_{v_2}(L,K,\pm)-E_{v_1}(L,K,\pm)=(v_2-v_1)(v_1+v_2+\alpha+K+1)\ , \tag{2.16a}$$

increases in proportion to $\sqrt{R}$ at large R. Similarly

TABLE I. The permissible values of the quantum number K, the symmetry label ($\pm$), and the corresponding values of α for several states ${}^{2S+1}L^{\pi}$.

${}^{2S+1}L^{\pi}$	Symmetry label	K	α	${}^{2S+1}L^{\pi}$	Symmetry label	K	α
${}^1S^e$	$+$	0	$\sqrt{R}$	${}^1F^e$	$-$	2	$\sqrt{4+R}$
${}^1P^o$	$-$	1	$\sqrt{R}$	${}^1F^o$	$-$	1	$\sqrt{5/2+R}$
					$-$	3	$\sqrt{3/2+R}$
${}^3P^e$	$+$	1	$\sqrt{1+R}$				
				${}^3F^e$	$+$	1	$\sqrt{17/2+R}$
${}^3P^o$	$+$	0	$\sqrt{1+R}$		$+$	3	$\sqrt{3/2+R}$
${}^1D^e$	$+$	0	$\sqrt{3+R}$	${}^3F^o$	$+$	0	$\sqrt{6+R}$
	$+$	2	$\sqrt{1+R}$		$+$	2	$\sqrt{4+R}$
${}^1D^o$	$+$	1	$\sqrt{4+R}$	${}^1G^e$	$+$	0	$\sqrt{10+R}$
					$+$	2	$\sqrt{8+R}$
${}^3D^e$	$-$	1	$\sqrt{1+R}$		$+$	4	$\sqrt{2+R}$
${}^3D^o$	$-$	2	$\sqrt{1+R}$				

$$E_{\nu_2}(L,K+2,\pm)-E_{\nu_1}(L,K,\pm)=(\nu_2-\nu_1)(\nu_1+\nu_2+K+1)+(2\nu_2+K+2)$$
$$+\tfrac{1}{2}(\alpha_2^2-\alpha_1^2)\pm L(L+1)\delta_{K1}+[(\nu_2+\tfrac{1}{2}K+\tfrac{3}{2})\alpha_2-(\nu_1+\tfrac{1}{2}K+\tfrac{1}{2})\alpha_1]\ . \tag{2.16b}$$

Note that $(\alpha_2^2-\alpha_1^2)$ does not depend on R and the only R dependence in (2.16b) comes from the last bracketed term. Thus the energy difference in (2.16b) also increases in proportion to $\sqrt{R}$ at large R unless $\nu_2=\nu_1-1$ in which case it goes to a constant value. This behavior of the energy difference will play a crucial role in Sec. II B.

B. The perturbations ΔH_1 and ΔH_2 in the large-R limit

Consider first the matrix element of ΔH_1 between the eigenfunctions of (H_0+V_M) defined in Sec. II A. It commutes with $L_{y'}$ and its matrix elements are diagonal in the index K. We evaluate the matrix element of the Coulomb interaction by using the finite series expansion derived from Eqs. (B2) and (B3) of Appendix B:

$$\langle \nu_2 LMK(\pm)\,|\,V_C\,|\,\nu_1 LMK(\pm)\rangle=\frac{R}{2}\left[\frac{\Gamma(\nu_1+K+1)}{\Gamma(\nu_1+1)}\frac{\Gamma(\nu_2+1)}{\Gamma(\nu_2+K+1)}\right]^{1/2}$$
$$\times\sum_{n=0}^{\nu_2}\frac{(-1)^n}{\Gamma(n+1)}\frac{\Gamma(\nu_1-n+\frac{1}{2})}{\Gamma(-n+\frac{1}{2})}\frac{1}{\Gamma(\nu_2-n+1)}G(\alpha)\ , \tag{2.17a}$$

where

$$G(\alpha)=(2\nu_1+\alpha+K+1)^{1/2}(2\nu_2+\alpha+K+1)^{1/2}\left[\frac{\Gamma(\nu_1+\alpha+K+1)}{\Gamma(\nu_1+\alpha+1)}\frac{\Gamma(\nu_2+\alpha+1)}{\Gamma(\nu_2+\alpha+K+1)}\right]^{1/2}$$
$$\times\frac{\Gamma(\alpha+n+\frac{1}{2})}{\Gamma(\nu_1+\alpha+K+n+\frac{3}{2})}\frac{\Gamma(\nu_2+n+\alpha+K+1)}{\Gamma(n+\alpha+1)}\ . \tag{2.17b}$$

We have assumed here that $\nu_1\geq\nu_2$ without any loss of generality. The following series expansion in powers of $1/\alpha$ is easily derived:

$$G(\alpha)=\frac{1}{\alpha^{\nu_1-\nu_2}}+[\nu_1-\tfrac{1}{2}(\nu_1-\nu_2)(\nu_1+\nu_2+K+2)-n(\nu_1-\nu_2+1)]\frac{1}{\alpha^{\nu_1-\nu_2+1}}+O(1/\alpha^{\nu_1-\nu_2+2})\ . \tag{2.18}$$

When (2.18) is substituted in (2.17a), the resulting series multiplying $1/\alpha^{\nu_1-\nu_2}$ is identified as a Gauss hypergeometric function of unit argument and the series multiplying $1/\alpha^{\nu_1-\nu_2+1}$ as the derivative of a similar function at $z=1$. This is sufficient to sum them, giving, for the typical element of V_C,

$$\langle \nu_2 LMK(\pm)\,|\,V_C\,|\,\nu_1 LMK(\pm)\rangle=(-1)^{\nu_1+\nu_2}\frac{R}{2}\frac{\Gamma(\frac{1}{2})}{\Gamma(\nu_1-\nu_2+1)\Gamma(\nu_2-\nu_1+\frac{1}{2})}\times\left[\frac{\Gamma(\nu_1+K+1)}{\Gamma(\nu_2+K+1)}\frac{\Gamma(\nu_1+1)}{\Gamma(\nu_2+1)}\right]^{1/2}$$
$$\times\left[\frac{1}{\alpha^{\nu_1-\nu_2}}-\tfrac{1}{2}(\nu_1-\nu_2-1)(\nu_1+\nu_2+K+1)\frac{1}{\alpha^{\nu_1-\nu_2+1}}+O(1/\alpha^{\nu_1-\nu_2+2})\right]$$
$$(\nu_1\geq\nu_2)\ . \tag{2.19}$$

Similarly, one can calculate the matrix element of the model interaction V_M:

$$\langle \nu_2 LMK(\pm) \mid V_M \mid \nu_1 LMK(\pm)\rangle = \frac{R}{4}\delta_{\nu_1\nu_2} + \frac{R}{4}\left[\frac{\Gamma(\nu_1+1)}{\Gamma(\nu_2+1)}\,\frac{\Gamma(\nu_1+K+1)}{\Gamma(\nu_2+K+1)}\right]^{1/2} G(\alpha)\ , \tag{2.20a}$$

with

$$G(\alpha) = \frac{1}{\alpha}(2\nu_1+\alpha+K+1)^{1/2}(2\nu_2+\alpha+K+1)^{1/2}\left[\frac{\Gamma(\nu_2+\alpha+1)}{\Gamma(\nu_1+\alpha+1)}\,\frac{\Gamma(\nu_2+\alpha+K+1)}{\Gamma(\nu_1+\alpha+K+1)}\right]^{1/2}\ , \tag{2.20b}$$

and the series expansion

$$G(\alpha) = \frac{1}{\alpha^{\nu_1-\nu_2}} - \tfrac{1}{2}(\nu_1-\nu_2-2)(\nu_1+\nu_2+K+1)\frac{1}{\alpha^{\nu_1-\nu_2+1}} + O(1/\alpha^{\nu_1-\nu_2+2})\ . \tag{2.20c}$$

Once again, Eq. (2.20) holds for $\nu_1 \geq \nu_2$ only.

Combining (2.19) and (2.20) we obtain

$$\begin{aligned}
&\langle \nu_2 LMK(\pm) \mid \Delta H_1 \mid \nu_1 LMK(\pm)\rangle \\
&\quad = -\frac{R}{4}\delta_{\nu_1\nu_2} + \frac{R}{4}\left[\frac{\Gamma(\nu_1+1)}{\Gamma(\nu_2+1)}\,\frac{\Gamma(\nu_1+K+1)}{\Gamma(\nu_2+K+1)}\right]^{1/2} \\
&\qquad \times \left[\left[(-1)^{\nu_1+\nu_2}\frac{2\Gamma(\frac{1}{2})}{\Gamma(\nu_1-\nu_2+1)\Gamma(\nu_2-\nu_1+\frac{1}{2})} - 1\right]\frac{1}{\alpha^{\nu_1-\nu_2}} \right. \\
&\qquad \left. - \left[(-1)^{\nu_1+\nu_2}\frac{(\nu_1-\nu_2-1)\Gamma(\frac{1}{2})}{\Gamma(\nu_1-\nu_2+1)\Gamma(\nu_2-\nu_1+\frac{1}{2})} - \tfrac{1}{2}(\nu_1-\nu_2-2)\right]\frac{(\nu_1+\nu_2+K+1)}{\alpha^{\nu_1-\nu_2+1}} \right] + O(R/\alpha^{\nu_1-\nu_2+2}) \quad (\nu_1 \geq \nu_2)\ .
\end{aligned} \tag{2.21}$$

When $\nu_1 = \nu_2$ or $\nu_1 = \nu_2 + 1$, the leading nonzero term in (2.21) is $O(R/\alpha^2)$ and when $\nu_1 \geq \nu_2 + 2$, the leading nonzero term is $O(R/\alpha^{\nu_1-\nu_2})$.

Thus the first-order corrections to the zeroth-order energies of (2.10) as well as the matrix elements on the first two super and subdiagonals ($\Delta\nu \leq 2$) go to a constant in the asymptotic limit $R \rightarrow \infty$. The remaining off-diagonal elements go to zero as $R^{(1-\Delta\nu/2)}$. Recall from (2.16a) that the separation between the zeroth-order energy levels increases as $\sqrt{R}$. The perturbation ΔH_1 may therefore be neglected in the asymptotic limit $R \rightarrow \infty$.

Next consider the matrix elements of the perturbation ΔH_2 [defined by Eq. (2.1d)] which obey the selection rule $|\Delta K| = 2$. Thus

$$\begin{aligned}
&\langle \nu_2 LM(K+2)(\pm) \mid \Delta H_2 \mid \nu_1 LMK(\pm)\rangle \\
&\quad = \tfrac{1}{16}[1+(\sqrt{2}-1)\delta_{K0}][(L-K-1)(L-K)(L+K+1)(L+K+2)]^{1/2} \\
&\qquad \times N_{\nu_2}^{\alpha_2,K+2} N_{\nu_1}^{\alpha_1,K} \int_{-1}^{1} d\xi\, P_{\nu_2}^{\alpha_2,K+2}(\xi)(1-\xi)^{(1/2)(\alpha_1+\alpha_2)-1}(1+\xi)^{K+2} P_{\nu_1}^{\alpha_1,K}(\xi)\ .
\end{aligned} \tag{2.22}$$

The integral in (2.22) can be reduced to the sum of a finite series by using (B2) and (B3). Here we are interested in the asymptotic value ($R \rightarrow \infty$) so that we can approximate $\alpha_1 = \alpha_2 = \alpha = \sqrt{R}$. The simpler integral

$$I = N_{\nu_2}^{\alpha,K+2} N_{\nu_1}^{\alpha,K} \int_{-1}^{1} d\xi\, P_{\nu_2}^{\alpha,K+2}(\xi)(1-\xi)^{\alpha-1}(1+\xi)^{K+2} P_{\nu_1}^{\alpha,K}(\xi)\ , \tag{2.23a}$$

can be reduced to a sum of three terms by twice using a recursion relation for the Jacobi polynomials (B1) and then the integral (B6). Since all the three terms are positive, we immediately obtain the following asymptotic formula:

$$\begin{aligned}
\lim_{\alpha\rightarrow\infty} I = \left[\frac{\Gamma(\nu_1+1)\Gamma(\nu_2+1)}{\Gamma(\nu_1+K+1)\Gamma(\nu_2+K+3)}\right]^{1/2} & \left[\left[\frac{\Gamma(\nu_>+K+3)}{\Gamma(\nu_<+1)}\,\frac{1}{\alpha^{\nu_>-\nu_<+2}}\right]_{\nu_1,\nu_2} \right. \\
& + \left[\frac{\Gamma(\nu_>+K+3)}{\Gamma(\nu_<+1)}\,\frac{2}{\alpha^{\nu_>-\nu_<+2}}\right]_{\nu_1-1,\nu_2} \qquad (2.23\text{b}) \\
& \left. + \left[\frac{\Gamma(\nu_>+K+3)}{\Gamma(\nu_<+1)}\,\frac{1}{\alpha^{\nu_>-\nu_<+2}}\right]_{\nu_1-2,\nu_2} \right]\ . \qquad (2.23\text{b})
\end{aligned}$$

In this equation $\nu_>(\nu_<)$ is the greater (lesser) of the two subscripts to the enclosing bracket.

Asymptotically, the matrix element (2.22) falls off at least as fast as $1/\alpha^2$ (i.e., as $1/R$). Recall from (2.16b) that the separation of the corresponding energy levels goes to a constant if $\nu_2 = \nu_1 - 1$, but increases as $\sqrt{R}$ otherwise. Therefore, the perturbation ΔH_2 also becomes negligible in the asymptotic limit $R \rightarrow \infty$.

As discussed earlier, the leading term in the first-order correction to the energy levels of (2.12) goes to a constant as

$R \to \infty$. We find

$$\Delta E^1 = \langle \nu LMK(\pm) \,|\, \Delta H_1 \,|\, \nu LMK(\pm) \rangle$$
$$= -\tfrac{1}{16}[4(2\nu+1)(\nu+K+1)+5\nu(\nu-1)](R/\alpha^2)$$
$$+O(R/\alpha^3) \; . \qquad (2.24)$$

One must add this term to the zeroth-order energy to obtain a result correct to R^0.

C. Transition from weak to strong correlation

We have diagonalized the Hamiltonian H_S of Eq. (1.2) for several values of R in the basis functions of (2.11a) as well as in the spherical-harmonic functions[13] previously used by Ezra and Berry.[3] The cumulative result of these computations is shown in Figs. 2(a) and 2(b) for even and odd parity states, respectively. For small radii ($R \leq 1$), we plot the energy (E) against the radius (R) whereas for $R \geq 1$ we take our cue from Eq. (2.10) and plot $E/\sqrt{R}$ against $\sqrt{R}$.

When $R \leq 1$, the energy depends linearly on R indicating that the Coulomb interaction between electrons is but a weak perturbation and the system is in the weak correlation regime. This regime may extend further than $R=1$, perhaps even substantially for some of the energy levels. What we wish to emphasize is that, as parametric functions of R, all states, regardless of parity, exhibit the same linear dependence and the same slope for the function $E/\sqrt{R}$ as a function of $\sqrt{R}$, so long as $\sqrt{R} \geq 4$. This behavior, which conforms with Eq. (2.10), characterizes the strong correlation regime. Moreover, in this regime (and in fact even at smaller R) a suitable zeroth-order basis function dominates overwhelmingly in the expansion of the exact wave function for all states considered. The *smallest* weight of the dominant basis function at $R=15$ for the energy levels shown in Fig. 2 is 91.2% and this quantity increases with increasing R.

It is curious, however, that even in the strong correlation regime the expansion in the zeroth-order functions of (2.11a) converges more slowly than the expansion in the spherical harmonic basis, i.e., given the same number of basis functions, the eigenvalues from the spherical harmonic basis are generally lower. (Of course, there is a much greater mixing of basis functions.) We believe the explanation lies in the relative inability of the zeroth-order basis to reproduce the exact wave function near $\xi=1$. Recall that the exact wave function possesses an expansion in powers of $(1-\xi)^{1/2}$ near $\xi=1$ [Eq. (2.4a)]. In particular, for the ${}^1S^e$, ${}^{1,3}P^o$, ${}^3P^e$, ${}^{1,3}D^o$, and ${}^3D^e$ states where there is no mixing between different K values for reasons of symmetry, the positive root s_1 of the indicial equation has the numerical values 0 for ${}^1S^e$ and ${}^1P^o$, $(\sqrt{2}-1)/2$ for ${}^3P^{o,e}$ and ${}^3D^{o,e}$ states, and $(\sqrt{5}-1)/2$ for ${}^1D^o$ states. In all these cases $0 \leq s_1 < 1$ and the wave function has a cusp at $\xi=1$. In contrast, the leading term in the power-series expansion of the zeroth-order functions is $(1-\xi)^{\alpha/2}$ where $\alpha \geq \sqrt{R}$. Consequently, at large R, the first several derivatives of these functions are zero and there is definitely no cusp at $\xi=1$. The spherical harmonic functions also do not have a cusp at $\xi=1$, but the leading term in their expansion $(1-\xi)^s$ has a power much less than $\sqrt{R}$ giving faster convergence.

It is shown in Fig. 2 that $R=13.7$ a.u., the radius which roughly corresponds to the $n=3$ intrashell states of helium, lies at the threshold of the strong correlation regime. We therefore expect that the energy levels and wave functions given by (2.10) and (2.11), with perhaps first-order corrections to the energies, will give a good approximation to the exact values. This is indeed so. In Fig. 3 we compare the approximate energy levels, including first-order corrections, with the numerical results of Ezra and Berry.[3] The agreement is excellent. In fact, the zeroth-order energy levels give good agreement too, especially for the rotor series ($\nu=0$, $K=0$), but we have not shown this to avoid cluttering the figure.

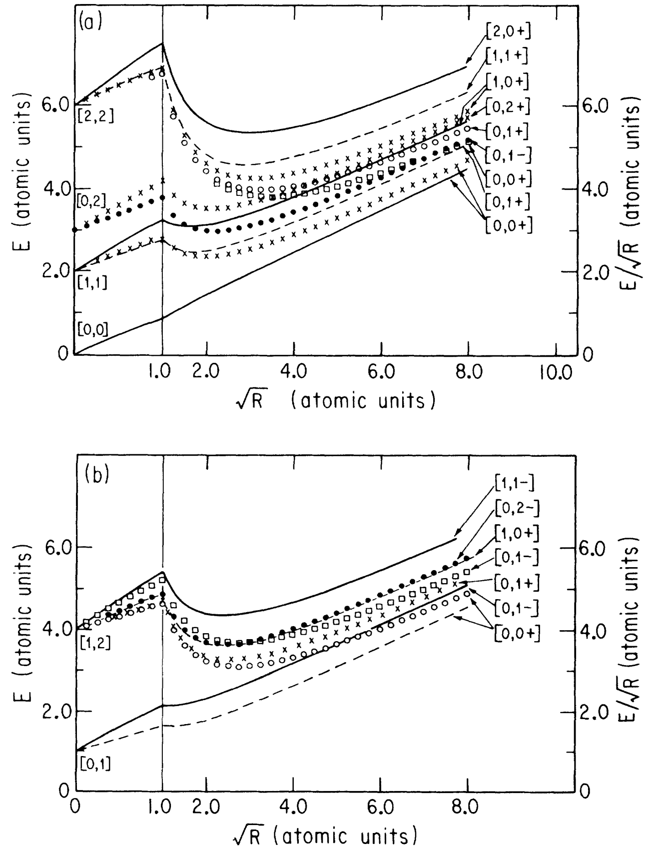

FIG. 2. The energy-level diagram for several states ${}^{2S+1}L^{\pi}$. Each figure is divided into two parts. In the left half ($0 \leq R \leq 1$) we plot the energy E against the radius R whereas in the right half ($\sqrt{R} \geq 1$), we plot $E/\sqrt{R}$ against $\sqrt{R}$. At $R=0$ the states are also labeled by the individual angular momenta of the electrons, whereas at large R the appropriate additional quantum numbers are $[\nu, K(\pm)]$. Note the nearly parallel lines of $E/\sqrt{R}$ vs R when $\sqrt{R} \geq 4$. (a) Even parity states: ${}^1S^e$(——), ${}^3P^e$(– – –), ${}^1D^e$(×), ${}^3D^e$(●), ${}^3F^e$(○), ${}^1G^e$(◇). (b) Odd parity states: ${}^1P^o$(——), ${}^3P^o$(– – –), ${}^1D^o$(×), ${}^3D^o$(●), ${}^3F^o$(○), ${}^1F^o$(◇).

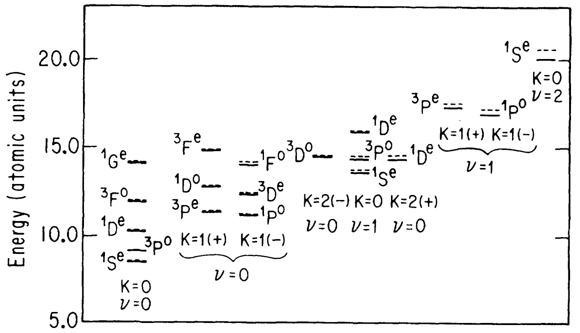

FIG. 3. A comparison of the approximate energy levels including first-order corrections (— — —) with the converged results of Ezra and Berry[3] (——) at $R=13.7$ a.u. Note that like Ezra and Berry we do not include the interaction with the nucleus and that we have scaled the Hamiltonian by R^2. The vibrational quantum number v_2 used by Ezra and Berry corresponds to $2\nu+K$.

The K doubling degeneracy for $K\geq 2$ is not lifted in first order. Thus the approximate $^3D^o[\nu=0,\ K=2\ (-)]$ level is degenerate with the $^1D^e[\nu=0,\ K=2\ (+)]$ level. However, the accidental degeneracy of these levels with the adjacent $^3P^o[\nu=1,\ K=0]$ level is lifted by the first-order correction.

In Fig. 4 we compare the approximate charge density distribution calculated from the zeroth-order wave functions of Eq. (2.11) with Ezra and Berry's calculation. Once again the agreement is excellent, particularly for the rotor series $[\nu=0,\ K=0]$. The only significant discrepancy is for the $^1D^e[\nu=0,\ K=2\ (+)]$ state near $\theta=\pi$. The approximate charge density is zero at $\theta=\pi$ because of the multiplicative factor $(1\text{-}\cos\theta)^K$ but the exact charge density is significantly large. The reason for this is that 13.7 a.u. is a sufficiently small radius for this state to mix significantly with the neighboring $^1D^e[\nu=1,\ K=0]$ state. [Recall from (2.16b) that the spacing of these levels goes to a constant as $R\rightarrow\infty$.] Accounting for this mixing goes a long way towards giving the correct charge density near $\theta=\pi$.

III. CONCLUDING REMARKS

In summary we have analyzed the nature of the angular correlation of two electrons on a sphere of radius R with particular regard to the transition from weakly correlated motion at small R to strongly correlated motion at large R. It is shown that in this limit the motion is indeed "molecular." However, the problem we have solved is only a model problem and ultimately it must justify itself by paving the way to the solution of the physically interesting problem with radially mobile electrons. A preliminary look suggests that carrying out a similar analysis of two electrons on concentric spheres of different radii is a little more difficult but feasible. In this case also, if the ratio R_2/R_1 (and correspondingly the angle $\chi=\arctan R_2/R_1$) is fixed and the hyperspherical radius $R=(R_1^2+R_2^2)^{1/2}$ is increased, the motion will evolve from being weakly correlated near $R\approx 0$ to being strongly correlated at $R\gg 1$. It is still a matter of speculation as to how to integrate our knowledge of the model systems into a treatment of electron correlation in doubly excited states of atoms. One path may be in the succession of steps developed for determining eigenfunctions and eigenvalues for rovibrational levels of triatomic molecules.[6] If it can be done, the results are likely to furnish insight into the connection between the molecular and hyperspherical pictures of strong correlation.[14]

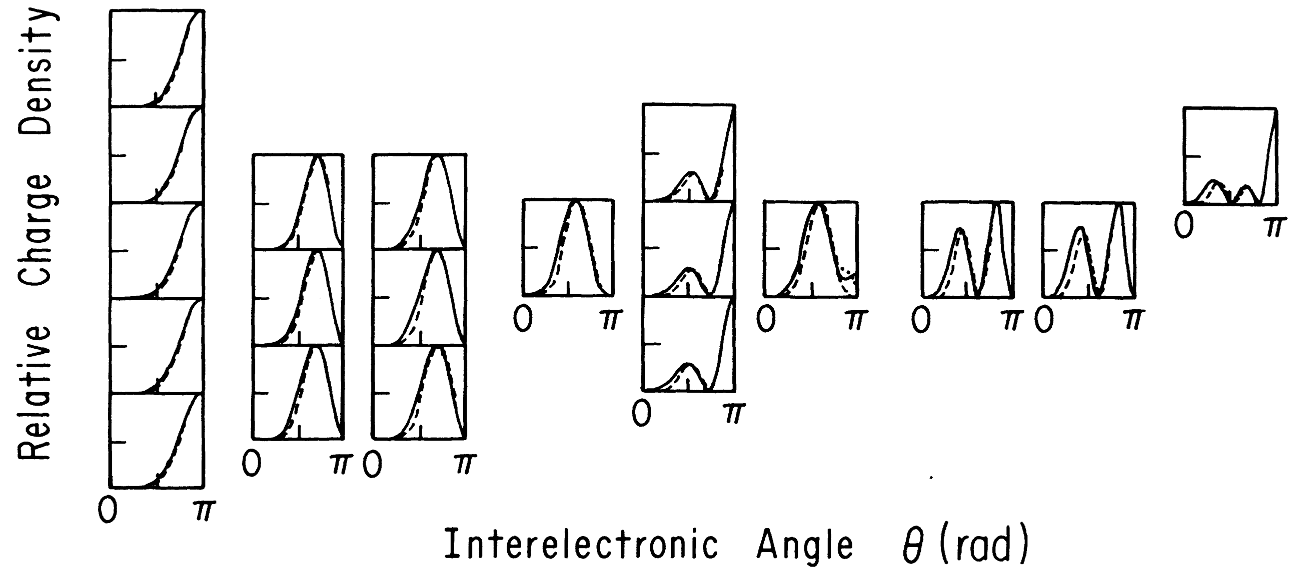

FIG. 4. A comparison between the approximate charge density calculated from (2.11a) (— — —) and the numerical result of Ezra and Berry (——). This figure is arranged in the same "supermultiplet" pattern as Fig. 3. The maximum in the charge density has been normalized to unity. The additional points (●) for the $^1D^e[\nu=1,\ K=1\ (-)]$ state near $\theta=\pi$ were calculated after allowing it to mix with the neighboring $^1D^e[\nu=1,\ K=0]$ state.

ACKNOWLEDGMENT

This research was supported by a grant from the National Science Foundation.

APPENDIX A: EULER ANGLE COORDINATES FOR TWO ELECTRONS

Since the present emphasis is on the collective motion of electrons, the most suitable system of coordinates consists of the angle θ between the radius vectors of the electrons, and the Euler angles (α,β,γ) which parametrize the orientation of the three body-fixed axes $(\hat{\mathbf{x}}',\hat{\mathbf{y}}',\hat{\mathbf{z}}')$ in the space-fixed frame $(\hat{\mathbf{x}},\hat{\mathbf{y}},\hat{\mathbf{z}})$. We use the bisector frame whose axes $(\hat{\mathbf{x}}',\hat{\mathbf{y}}',\hat{\mathbf{z}}')$ are defined by

$$\hat{\mathbf{x}}'=\frac{\hat{\mathbf{r}}_1+\hat{\mathbf{r}}_2}{|\hat{\mathbf{r}}_1+\hat{\mathbf{r}}_2|},\quad \hat{\mathbf{y}}'=\hat{\mathbf{z}}'\times\hat{\mathbf{x}}',\quad \hat{\mathbf{z}}'=\frac{\hat{\mathbf{r}}_1\times\hat{\mathbf{r}}_2}{|\hat{\mathbf{r}}_1\times\hat{\mathbf{r}}_2|}, \tag{A1}$$

where $\hat{\mathbf{r}}_1=\mathbf{r}_1/r_1$ and $\hat{\mathbf{r}}_2=\mathbf{r}_2/r_2$ are the unit vectors along the directions of the electrons. A sequence of three rotations takes the space-fixed frame into the body-fixed frame:[8]

$$\begin{bmatrix}\hat{\mathbf{x}}'\\ \hat{\mathbf{y}}'\\ \hat{\mathbf{z}}'\end{bmatrix}=\mathcal{R}_{\hat{\mathbf{z}}'}(\gamma)\mathcal{R}_{\hat{\mathbf{y}}''}(\beta)\mathcal{R}_{\hat{\mathbf{z}}}(\alpha)\begin{bmatrix}\hat{\mathbf{x}}\\ \hat{\mathbf{y}}\\ \hat{\mathbf{z}}\end{bmatrix}. \tag{A2}$$

The subscript to each rotation operator denotes its instantaneous axis of rotation. Equation (A2) defines the Euler angles (α,β,γ). In this representation the angular momentum operators are given explicitly as follows:

$$L_x=-i\left[-\cos\alpha\cot\beta\frac{\partial}{\partial\alpha}-\sin\alpha\frac{\partial}{\partial\beta}+\frac{\cos\alpha}{\sin\beta}\frac{\partial}{\partial\gamma}\right], \tag{A3a}$$

$$L_y=-i\left[-\sin\alpha\cot\beta\frac{\partial}{\partial\alpha}+\cos\alpha\frac{\partial}{\partial\beta}+\frac{\sin\alpha}{\sin\beta}\frac{\partial}{\partial\gamma}\right], \tag{A3b}$$

$$L_z=-i\frac{\partial}{\partial\alpha}, \tag{A3c}$$

$$L^2=-\frac{1}{\sin\beta}\frac{\partial}{\partial\beta}\sin\beta\frac{\partial}{\partial\beta}-\frac{1}{\sin^2\beta}\left[\frac{\partial^2}{\partial\alpha^2}-2\cos\beta\frac{\partial^2}{\partial\alpha\partial\gamma}+\frac{\partial^2}{\partial\gamma^2}\right]. \tag{A4}$$

The raising and lowering operators for L_z are, as usual $L_\pm=L_x\pm iL_y$. The following operators are the projections of the angular momentum on the body-fixed axes:

$$L_{x'}=-i\left[\cot\beta\cos\gamma\frac{\partial}{\partial\gamma}-\frac{\cos\gamma}{\sin\beta}\frac{\partial}{\partial\alpha}+\sin\gamma\frac{\partial}{\partial\beta}\right], \tag{A5a}$$

$$L_{y'}=-i\left[-\cot\beta\sin\gamma\frac{\partial}{\partial\gamma}+\frac{\sin\gamma}{\sin\beta}\frac{\partial}{\partial\alpha}+\cos\gamma\frac{\partial}{\partial\beta}\right], \tag{A5b}$$

$$L_{z'}=-i\frac{\partial}{\partial\gamma}. \tag{A5c}$$

These satisfy the commutation rules of the "reverse" angular momentum,

$$[L_{x'},L_{y'}]=-iL_{z'},\quad [L_{y'},L_{z'}]=-iL_{x'},\quad [L_{z'},L_{x'}]=-iL_{y'}, \tag{A6a}$$

and consequently, the raising and lowering operators for $L_{z'}$ are

$$L'_\pm=-L_{x'}\pm iL_{y'}. \tag{A6b}$$

Moreover, all operators L_x,L_y,L_z commute with $(L_{x'},L_{y'},L_{z'})$. The operators L^2, L_z, and $L_{z'}$, can be diagonalized simultaneously, and their eigenfunctions are the Wigner rotation matrices $\mathcal{D}^L_{MK}(\alpha\beta\gamma)$ such that

$$L^2\mathcal{D}^L_{MK}(\alpha\beta\gamma)=L(L+1)\mathcal{D}^L_{MK}(\alpha\beta\gamma), \tag{A7a}$$

$$L_z\mathcal{D}^L_{MK}(\alpha\beta\gamma)=M\mathcal{D}^L_{MK}(\alpha\beta\gamma), \tag{A7b}$$

$$L_{z'}\mathcal{D}^L_{MK}(\alpha\beta\gamma)=K\mathcal{D}^L_{MK}(\alpha\beta\gamma). \tag{A7c}$$

The rotation matrices themselves are

$$\mathcal{D}^L_{MK}(\alpha\beta\gamma)=\left[\frac{1}{\sqrt{2\pi}}e^{iM\alpha}\right]\left[\frac{1}{\sqrt{2\pi}}e^{iK\gamma}\right](-1)^{1/2[K-M+|K-M|]}N^{\mu',\mu}_\nu(1-\cos\beta)^{\mu'/2}(1+\cos\beta)^{\mu/2}P^{\mu',\mu}_\nu(\cos\beta), \tag{A8a}$$

where $\mu'=|K-M|$, $\mu=|K+M|$, $\nu=L-\frac{1}{2}(\mu'+\mu)$, and

$$N^{\mu',\mu}_\nu=\left[\frac{(2\nu+\mu'+\mu+1)}{2^{\mu'+\mu+1}}\frac{\Gamma(\nu+1)}{\Gamma(\nu+\mu+1)}\frac{\Gamma(\nu+\mu'+\mu+1)}{\Gamma(\nu+\mu'+1)}\right]^{1/2} \tag{A8b}$$

is the normalization factor for the Jacobi polynomial $P^{\mu',\mu}_\nu(\cos\beta)$. The choice of the phase factor in the definition of the rotation matrices ensures that no such factors appear on the action of the raising and lowering operators $L_\pm$ and $L'_\pm$. Thus

$$L_\pm\mathcal{D}^L_{MK}(\alpha\beta\gamma)=[(L\mp M)(L\pm M+1)]^{1/2}\mathcal{D}^L_{M\pm 1K}(\alpha\beta\gamma), \tag{A9a}$$

and

$$L'_\pm\mathcal{D}^L_{MK}(\alpha\beta\gamma)=[(L\mp K)(L\pm K+1)]^{1/2}\mathcal{D}^L_{MK\pm 1}(\alpha\beta\gamma). \tag{A9b}$$

The operation of inversion $\hat{I}_{\mathrm{op}}$ or $(\mathbf{r}_1,\mathbf{r}_2)\rightarrow(-\mathbf{r}_1,-\mathbf{r}_2)$, implies $(\alpha,\beta,\gamma)\rightarrow(\alpha,\beta,\gamma+\pi)$. Evidently,

$$\hat{I}_{\mathrm{op}}\mathcal{D}^L_{MK}(\alpha\beta\gamma)=(-1)^K\mathcal{D}^L_{MK}(\alpha\beta\gamma). \tag{A10a}$$

Next we examine exchange symmetry. The electrons must be exchanged in the space-fixed frame before making the transformation to the rotating frame. Then $(\mathbf{r}_1 \rightleftarrows \mathbf{r}_2)$ implies $(\alpha,\beta,\gamma) \to (\alpha-\pi,\pi-\beta,2\pi-\gamma)$, $r_1 \rightleftarrows r_2$, and $\theta \to \theta$. Consequently, on permutation

$$P_{12}\mathcal{D}^L_{MK}(\alpha\beta\gamma) = (-1)^L \mathcal{D}^L_{M-K}(\alpha\beta\gamma) \ . \tag{A10b}$$

In this paper we use an alternative set of mutually commuting operators L^2, L_z, and $L_{y'}$. The corresponding eigenfunctions are denoted $|LMK\rangle_{y'}$ with an obvious interpretation of the quantum numbers. These may be generated by rotating $|LMK\rangle_{z'}$ by $\pi/2$ about the $\hat{\mathbf{x}}'$ axis:

$$|LMK\rangle_{y'} = \exp\left[-i\frac{\pi}{2}L_{x'}\right]|LMK\rangle_{z'} \ . \tag{A11a}$$

The most convenient raising and lowering operators for these functions are obtained by a cyclic permutation of (A6b) followed by multiplication by $\pm i$. Then

$$(-L_{x'} \mp iL_{z'})|LMK\rangle_{y'} = [(L \mp K)(L \pm K + 1)]^{1/2}|LMK \pm 1\rangle_{y'} \ . \tag{A11b}$$

These functions transform as follows under inversion and exchange:

$$\hat{I}_{\text{op}}|LMK\rangle_{y'} = (-1)^{L+K}|LM-K\rangle_{y'} \ , \tag{A11c}$$

and

$$P_{12}|LMK\rangle_{y'} = (-1)^L|LMK\rangle_{y'} \ . \tag{A11d}$$

Normalized functions of definite parity and exchange symmetry (when $K \neq 0$) may be constructed by taking symmetric and antisymmetric combinations of $|LMK\rangle_{y'}$ and $|LM-K\rangle_{y'}$:

$$|LMK(\pm)\rangle = \frac{1}{\sqrt{2}}[\,|LMK\rangle \pm |LM-K\rangle], \quad K \neq 0 \ . \tag{A12a}$$

Then,

$$\hat{I}_{\text{op}}|LMK(\pm)\rangle = (-1)^{L+K+\binom{0}{1}}|LMK(\pm)\rangle_{y'} \ , \tag{A12b}$$

and

$$P_{12}|LMK(\pm)\rangle = (-1)^{L+\binom{0}{1}}|LMK(\pm)\rangle_{y'} \ . \tag{A12c}$$

We will also need explicit expressions for the operators l^2 and $\mathbf{L}\cdot\boldsymbol{l}$ (where $\mathbf{L} = \boldsymbol{l}_1 + \boldsymbol{l}_2, \boldsymbol{l} = \boldsymbol{l}_1 - \boldsymbol{l}_2$) in the coordinates $(\xi = \cos\theta, \alpha, \beta, \gamma)$

$$l^2 = -4(1-\xi^2)\frac{d^2}{d\xi^2} + 8\xi\frac{d}{d\xi} + \frac{(1+\xi)}{(1-\xi)}L_{x'}^2 + \frac{(1-\xi)}{(1+\xi)}L_{y'}^2 \ , \tag{A13a}$$

and

$$\mathbf{L}\cdot\boldsymbol{l} = \frac{1}{(1-\xi^2)^{1/2}}\left[i\left[-(1-\xi^2)\frac{d}{d\xi} + \frac{\xi}{2}\right]L_{x'} - \tfrac{1}{2}(L_{x'}L_{y'} + L_{y'}L_{x'}) \right] \ . \tag{A13b}$$

In the main body of the paper we use the functions $|LMK(\pm)\rangle_{y'}$ but the subscript y' has been dropped.

APPENDIX B: SOME USEFUL MATHEMATICAL RESULTS

The following recursion relation for the Jacobi polynomials has been used in the text:[12]

$$(2\nu+\alpha+\beta)P_\nu^{\alpha,\beta-1}(\xi) = (\nu+\alpha+\beta)P_\nu^{\alpha,\beta}(\xi) + (\nu+\alpha)P_{\nu-1}^{\alpha,\beta}(\xi) \ . \tag{B1}$$

An expansion in powers of $(1-\xi)$ is useful for calculating integrals:

$$P_\nu^{\alpha,\beta}(\xi) = \frac{\Gamma(\nu+\alpha+1)}{\Gamma(\nu+\alpha+\beta+1)} \sum_{n=0}^{\nu} \frac{\Gamma(\nu+\alpha+\beta+1+n)}{\Gamma(\alpha+1+n)\Gamma(n+1)\Gamma(\nu-n+1)}[(\xi-1)/2]^n \ . \tag{B2}$$

The basic integral we use has been tabulated by Gradshteyn and Ryzhik:[15]

$$\int_{-1}^{1} d\xi(1-\xi)^\rho(1+\xi)^\beta P_\nu^{\alpha,\beta}(\xi) = \frac{2^{\rho+\beta+1}\Gamma(\rho+1)\Gamma(\nu+\beta+1)\Gamma(\alpha-\rho+\nu)}{\Gamma(\nu+1)\Gamma(\alpha-\rho)\Gamma(\nu+\rho+\beta+2)}, \quad \text{Re}\rho > -1, \quad \text{Re}\beta > -1 \ . \tag{B3}$$

Using (B2) and (B3) we can show that

$$\begin{aligned}\int_{-1}^{1} d\xi\, P_{\nu_1}^{\alpha,\beta}(\xi)(1-\xi)^\rho(1+\xi)^\beta P_{\nu_2}^{\alpha,\beta}(\xi) &= 2^{\rho+\beta+1}\frac{\Gamma(\nu_1+\beta+1)\Gamma(\nu_2+\alpha+1)}{\Gamma(\nu_1+1)\Gamma(\nu_2+\alpha+\beta+1)} \\ &\quad \times \sum_{n=0}^{\nu_2}(-1)^n \frac{\Gamma(\nu_2+\alpha+\beta+1+n)\Gamma(n+\rho+1)\Gamma(\nu_1+\alpha-n-\rho)}{\Gamma(\alpha+1+n)\Gamma(1+n)\Gamma(\nu_2-n+1)\Gamma(\alpha-\rho-n)\Gamma(\nu_1+\rho+\beta+2+n)} \ .\end{aligned} \tag{B4}$$

This result is valid for all ν_1 and ν_2 but in the following we will assume that $\nu_1 \geq \nu_2$. Note that

$$\frac{\Gamma(\nu_1+\alpha-n-\rho)}{\Gamma(\alpha-n-\rho)} = (\alpha-\rho-n)_{\nu_1} = (\alpha-\rho-n)(\alpha-\rho-n+1)\cdots(\alpha-\rho-n+\nu_1-1) \ .$$

When $\rho = \alpha$, and $\nu_1 > \nu_2$, this term is zero for all values of n and the integral is zero. However, when $\nu_1 = \nu_2$, a nonzero contribution to the sum arises from the $n=\nu_2$ term, and one obtains the normalization integral for the Jacobi polynomials:

$$\int_{-1}^{1} d\xi\, P_{\nu_1}^{\alpha,\beta}(\xi)(1-\xi)^{\alpha}(1+\xi)^{\beta}P_{\nu_2}^{\alpha,\beta}(\xi)=\delta_{\nu_1\nu_2}\frac{2^{\alpha+\beta+1}}{(2\nu_1+\alpha+\beta+1)}\frac{\Gamma(\nu_1+\beta+1)\Gamma(\nu_1+\alpha+1)}{\Gamma(\nu_1+1)\Gamma(\nu_1+\alpha+\beta+1)} . \tag{B5}$$

The case $\rho=\alpha-1$ will be of special interest to us. Then the only nonzero contribution in (B4) comes from the $n=0$ term. Thus

$$\int_{-1}^{1} d\xi\, P_{\nu_1}^{\alpha,\beta}(\xi)(1-\xi)^{\alpha-1}(1+\xi)^{\beta}P_{\nu_2}^{\alpha,\beta}(\xi)=\frac{2^{\alpha+\beta}}{\alpha}\frac{\Gamma(\nu_1+\beta+1)\Gamma(\nu_2+\alpha+1)}{\Gamma(\nu_2+1)\Gamma(\nu_1+\alpha+\beta+1)}, \quad \nu_1\geq\nu_2 . \tag{B6}$$

---

[1] M. E. Kellman and D. R. Herrick, J. Phys. B **11**, L755 (1978); Phys. Rev. A **22**, 1536 (1980); D. R. Herrick and M. E. Kellman, *ibid.* **21**, 418 (1980); D. R. Herrick, M. E. Kellman, and R. D. Poliak, *ibid.* **22**, 1517 (1980).

[2] G. S. Ezra and R. S. Berry, Phys. Rev. A **28**, 1974 (1983); J. L. Krause and R. S. Berry, J. Chem. Phys. **83**, 5153 (1985); Phys. Rev. A **31**, 3502 (1985); Comments At. Mol. Phys. **18**, 91 (1986).

[3] G. S. Ezra and R. S. Berry, Phys. Rev. A **25**, 1513 (1982).

[4] G. S. Ezra and R. S. Berry, Phys. Rev. A **28**, 1989 (1983).

[5] S. I. Nikitin and V. N. Ostrovsky, J. Phys. B **18**, 4349 (1985); **18**, 4371 (1985).

[6] G. A. Natanson, G. S. Ezra, G. Delgado-Barrio, and R. S. Berry, J. Chem. Phys. **81**, 3400 (1984); **84**, 2035 (1986).

[7] We found it difficult to use directly the results given in Ref. 5 or in the article by A. K. Bhatia and A. Temkin, Rev. Mod. Phys. **36**, 1050 (1964). We have therefore summarized the definition of the Euler angles, the representation of the angular momentum operators, and the properties of the eigenfunctions in Sec. II without attempting to prove the results. The proofs are based on standard techniques which can be found in any book on the quantum theory of angular momentum.

[8] A useful pictorial representation of the transformation is given in A. R. Edmonds, *Angular Momentum in Quantum Mechanics* (Princeton University Press, Princeton, New Jersey, 1960).

[9] The quantum number K which we use may be veiwed alternatively as the "vibrational angular momentum" arising from a superposition of two degenerate bending vibrations. It corresponds to the quantum number l used by Ezra and Berry (Ref. 3). The quantum number v_2 used by Ezra and Berry corresponds to the combination $2\nu+K$ in our notation.

[10] These are discussed in A. Erdélyi, *Higher Transcendental Functions* (McGraw-Hill, New York, 1955), Vol. III, p. 57. The solution by expansion in an infinite set of Jacobi polynomials is discussed further by A. Erdélyi, Duke Math. J. **9**, 48 (1942); Quart. J. Math. Oxford Ser. **15**, 62 (1944).

[11] A. Erdélyi, *Higher Transcendental Functions* (McGraw-Hill, New York, 1953), Vol. II.

[12] We follow the convention of M. Abramowitz and I. A. Stegun, *Handbook of Mathematical Functions* (National Bureau of Standards, Washington, D.C., 1964).

[13] More precisely, these are antisymmetrized and angular momentum coupled products of two spherical harmonics.

[14] This is of course a topic of much current interest. The reader may wish to consult C. D. Lin, Phys. Rev. Lett. **51**, 1348 (1983); Phys. Rev. A **29**, 1019 (1984); S. Watanabe and C. D. Lin, *ibid.* **34**, 823 (1986); J. M. Feagin and J. S. Briggs, Phys. Rev. Lett. **57**, 984 (1986).

[15] I. S. Gradshteyn and Ryzhik, *Table of Integrals, Series and Products* (Academic, New York, 1980).